HHS Public Access

Author manuscript

Curr Biol. Author manuscript; available in PMC 2017 December 05.

Published in final edited form as:

Curr Biol. 2016 December 05; 26(23): 3116–3128. doi:10.1016/j.cub.2016.09.038.

The TRP channels Pkd2, NompC and Trpm act in cold-sensing neurons to mediate unique aversive behaviors to noxious cold in *Drosophila*

Heather N. Turner[1,2,7], **Kevin Armengol**[4,7,11], **Atit A. Patel**[5], **Nathaniel J. Himmel**[5], **Luis Sullivan**[4,8], **Srividya Chandramouli Iyer**[4,9], **Surajit Bhattacharya**[5], **Eswar Prasad R. Iyer**[4,10], **Christian Landry**[6], **Michael J. Galko**[1,2,3,7,*], and **Daniel N. Cox**[4,5,7,*]

[1]Department of Genetics; University of Texas MD Anderson Cancer Center; Houston, TX, 77030; USA

[2]Neuroscience Program, Graduate School of Biomedical Sciences; Houston, TX, 77030; USA

[3]Genes and Development Program, Graduate School of Biomedical Sciences; Houston, TX, 77030; USA

[4]School of Systems Biology; Krasnow Institute for Advanced Study; George Mason University; Fairfax, VA, 22030; USA

[5]Neuroscience Institute; Georgia State University; Atlanta, GA, 30303; USA

[6]ProDev Engineering; Missouri City, TX, 77459; USA

SUMMARY

The basic mechanisms underlying noxious cold perception are not well understood. We developed *Drosophila* assays for noxious cold responses. Larvae respond to near-freezing temperatures via a mutually exclusive set of singular behaviors–in particular, a full body contraction (CT). Class III (CIII) multidendritic sensory neurons are specifically activated by cold and optogenetic activation of these neurons elicits CT. Blocking synaptic transmission in CIII neurons inhibits CT. Genetically, the transient receptor potential (TRP) channels Trpm, NompC, and Polycystic kidney

[*]Correspondence: Michael J. Galko (mjgalko@mdanderson.org) and Daniel N. Cox (dcox18@gsu.edu).
[7]These authors contributed equally to this work
[8]Present address: Institute of Neuroscience; University of Oregon; Eugene, OR, 97403; USA
[9]Present address: Whitehead Institute for Biomedical Research; MIT; Cambridge, MA, 02142; USA
[10]Present address: Wyss Institute; Harvard Medical School; Cambridge, MA, 02115; USA
[11]Present address: Department of Biology; University of Maryland; College Park, MD, 20742; USA

AUTHOR CONTRIBUTIONS

Writing – Original Draft: H.N.T. and M.J.G.; *Writing – Review & Editing:* H.N.T., M.J.G., K.A., A.A.P. and D.N.C.; *Conceptualization:* H.N.T., M.J.G., K.A., A.A.P. and D.N.C.; *Investigation: H.N.T. cold probe and gentle touch assays; K.A. cold plate assays, GCaMP6 imaging, optogenetics, and morphology analyses; A.A.P. cold plate analyses, GCaMP6 and CaMPARI imaging, optogenetic dose-response, qRT-PCR analyses and contributed to morphology analyses; N.J.H. cold plate analyses and optogenetic dose-response; L.S. contributed to cold plate assay development and data; S.C.I. CIII neuron microarrays; S.B. bioinformatic analyses of microarray data; E.P.R.I. contributed to development GCaMP6 imaging and identified the CII GAL4 driver used in this study; C.L. designed and engineered the cold probe; All authors critically read and commented on the final version of the manuscript.*

disease 2 (Pkd2) are expressed in CIII neurons where each is required for CT. Misexpression of *Pkd2* is sufficient to confer cold-responsiveness. The optogenetic activation level of multimodal CIII neurons determines behavioral output, and visualization of neuronal activity supports this conclusion. Coactivation of cold and heat responsive sensory neurons suggests that the cold-evoked response circuitry is dominant. Our *Drosophila* model will enable a sophisticated molecular genetic dissection of cold nociceptive genes and circuits.

Graphical abstract

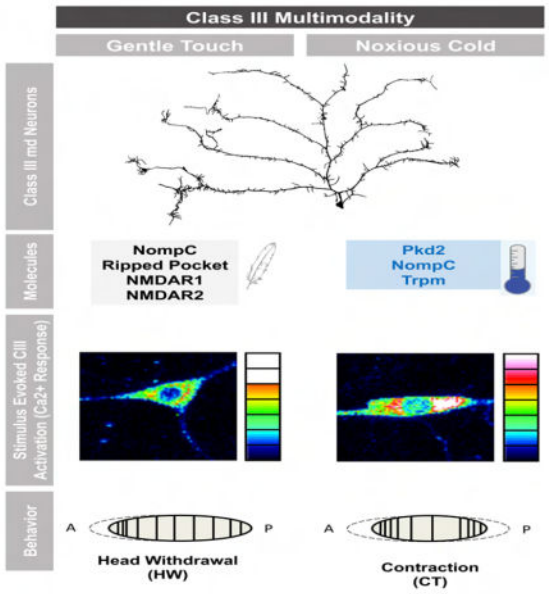

INTRODUCTION

Diverse animals respond to noxious cold with stereotyped behaviors, which mostly reduce the tissue surface area exposed to low temperature. Such responses occur in endotherms [1, 2] and ectotherms [3], highlighting the importance of maintaining a healthy body temperature. The assays used to assess responses to noxious cold in laboratory animal models include the cold plate [4], tail flick [5], and exposure to acetone [6] or dry ice [7]. Although all are useful for analyzing genes implicated in cold nociception in rodents [8, 9], the field has lacked a genetically tractable system where unbiased forward genetic identification of cold nociception genes is both feasible and cost effective. *Drosophila* possess powerful genetic tools for analyzing genes and neural pathways [10] and have recently identified conserved players in thermal and mechanical nociception and nociceptive sensitization [11–14]. Although prolonged exposure to temperatures 10 ºC and below is fatal [15], how *Drosophila* larvae respond to acute noxious cold stimuli is currently unknown.

The *Drosophila* larval peripheral nervous system has four classes of type II multiple dendritic (md) sensory neurons that innervate the barrier epidermis. Each class has its own stereotypic location, dendritic arbor territory and morphology [16]. Class IV (CIV) neurons respond to noxious heat [17] and mechanical [13, 17, 18] stimuli and mediate aversive

rolling. Class II (CII) and class III (CIII) neurons mediate gentle touch responses [19, 20]. All md neurons possess naked nerve endings, similar to cold-responsive non-myelinated C fibers in vertebrates [16]. Myelinated peripheral Aδ fibers also contribute to these responses [21]. It is not known which peripheral neuron class(es) are cold-sensitive, if any, in *Drosophila*.

TRP channels are variably selective cation channels containing multiple subunits and six transmembrane domains. TRP channels function ubiquitously in sensory biology, including nociception [22]. Vertebrate TRPV1 responds to noxious heat in skin [23] while Painless (a TRPA channel) is required for aversive rolling to noxious touch and heat in flies [24]. However, the cells and channels required for responding to cold have been difficult to pinpoint. TRPM8 detects both innocuous and noxious cold in rat peripheral sensory neurons [25]. TRPA1 has also been implicated as a vertebrate noxious cold receptor [26], however some cold sensing neurons do not express TRPM8 or TRPA1 [27], suggesting alternative noxious cold channels exist. Thermal preference assays in *C. elegans* have also identified genes responsible for cool sensing [28]. In *Drosophila* larvae, collective studies implicate *trp, trpl* and *iav* in cool avoidance (10–20 °C) [29, 30] and the TRPP-like *brivido* channel senses cool temperatures (12–15 °C) in adult flies [31]. Although *Drosophila* TRP channels are clearly involved in cool avoidance, whether they are also involved in acute noxious cold (≤ 10 °C) sensing is unknown.

Using global and local cold assays we investigated the cellular and molecular bases of cold nociception in *Drosophila* larvae. Acute noxious cold provoked a set of unique behaviors with a full body contraction (CT) as the primary response. The strongest and most specific calcium responses to cold were found in CIII md neurons. Additionally, direct optogenetic activation of CIII neurons in the absence of cold, caused CT while silencing CIII neurons attenuated responses to cold. The TRP channels NompC, Trpm and Pkd2 play key roles in cold nociception in CIII neurons. Interestingly, the level of activation of CIII neurons determined whether the output response was a light touch or cold-evoked behavior. Consistent with this, light touch and cold activated CIII neurons to different extents. Finally, coactivation of CIII and CIV (heat/mechanical) neurons evoked CT at the expense of aversive rolling, providing insight into nociceptive circuit organization. Our findings reveal that *Drosophila* use a distinct set of cells, channels and aversive behaviors to respond to extreme cold.

RESULTS

Drosophila larvae contract in response to noxious cold

To determine how *Drosophila* larvae respond to noxious [15] cold, we developed two complementary behavioral assays. One involves global contact along the ventral body surface (Figure 1A) and the second involves a local noxious cold stimulus (Figure 1C). In the global assay, larvae were acclimated to a 25 ºC metal plate (Movie S1), then transferred to a cold or cool surface (4–16 °C) (Figure 1A). Two unique behaviors were observed, distinct from normal peristaltic locomotion (Movie S1), gentle touch behaviors [32, 33], and aversive rolling to noxious heat [11, 24] or force [13, 17, 18, 24]. The cold-evoked behaviors were a 45–90 ° head and/or tail raise (HTR) or a contraction (CT) of the head and tail

towards the middle of the body (Movie S2). 14 ºC and below CT was the predominant response, increasing with decreasing temperature (peak at 4 ºC), while HTR responses peaked at 10 ºC (Figure 1B).

Given that cold-induced muscular contractions [34] might induce CT in the global assay, we constructed a cold probe for locally stimulating larvae from ambient temperatures to 3 °C (Figure 1C). The cold probe-evoked behaviors were: 1. CT, identical to the global assay; 2. A 45–90 ° simultaneous head and posterior raise (US for U-shape); and 3. A 45–90 ° raise of the posterior body segments (PR for posterior raise); US and PR being similar to individual HTR behaviors observed in the global assay (Movie S3). These behaviors were not observed during normal locomotion but their frequencies increased upon stimulation with decreasing temperatures (Figure 1D). Each behavior had a unique response versus temperature curve. US and PR exhibited broad peaks between 3–8 °C, while CT peaked between 9–14 °C (Figures S1A-S1C). CT was the only behavior occasionally observed in response to light touch (Figure 1D; Figure S1C). As with heat [11, 24], the average response latency decreased with decreasing temperature (Figure S1D). Since CT arises from the focal (one body segment) application of cold, CT is not likely due to global cold-induced muscle contraction.

To determine if there were three distinct classes of responders (CT, US, PR), we retested larvae after an arbitrary 20-minute period. Larvae did not consistently reproduce their initial behavior, although there was a slight preference for reproducing CT (Figure S1E). This ruled out three distinct responder classes. To test whether slight differences in the placement of the cold probe could affect behavioral output, we systematically varied the probe position along the anteroposterior axis. Positioning the probe one or two segments closer to the head (region 2) or posterior spiracles (region 4) had no significant effect on US or CT (Figure S1F). However, cold stimulation directly to the head (region 1) resulted in a dramatic increase in CT, while stimulation to the tail (region 5) resulted in fewer responders (Figure S1F).

The results from the global and local assays indicate that *Drosophila* larvae exhibit a unique set of behaviors in response to noxious cold that are distinct from normal locomotion, light touch responses, and aversive rolling to noxious heat or mechanical stimuli.

Cold stimulation results in specific Ca^{2+} responses within class III md neurons

To investigate if md neurons display Ca^{2+} responses to cold stimulation (6 °C), we live-imaged intact third instar larvae expressing GCaMP6 in md neurons (Figure S2A). Compared to their respective baselines, cold stimulation produced a slight increase in GCaMP6 signals in class I (CI) and a moderate increase in CII neurons (Figures 2A–2B). By contrast, CIII neurons showed a robust increase in GCaMP6 fluorescence (Figure 2C; Movie S4). Heat-responsive CIV neurons were largely inert to cold (Figure 2D). Statistical comparisons of average peak GCaMP6 signals demonstrated significantly higher peak fluorescence levels in CIII neurons relative to the other subclasses (Figure S2B; Figure 2E). To assess the specificity of GCaMP6 signals in md neuron subtypes as a function of temperature, we compared their average max changes in GCaMP fluorescence from ambient to cold temperatures and performed cross-correlation analyses (Figure 2F; Figure S2C). A

strong negative cross-correlation coefficient was observed in CIII neurons at lower temperatures (Figure 2F; Movie S4) and they were not significantly activated by noxious heat stimulation (44 ºC) (Figure S2D), indicating cold specificity. Noxious heat stimulation does not inactivate GCaMP6 because heat followed by subsequent noxious cold still gave a robust CIII GCaMP6 signal (Figures S2D–S2E). Together, these results demonstrate that CIII, and to a lesser extent CII, neurons are cold-activated.

Optogenetic activation of class III md neurons causes CT behavior

Cold-evoked Ca^{2+} responses observed in CIII neurons led us to ask whether direct optogenetic activation of these neurons, in the absence of cold, would elicit cold-specific behaviors. Larvae expressing the ultrafast Channelrhodopsin-2 variant ChETA in CIII neurons or in other md classes (Figure S3) were stimulated with high intensity blue light with or without all *trans*-retinal (ATR, a required cofactor for ChETA function). In controls, most larvae continued normal locomotion and a few displayed HTR behavior upon light exposure (Figure S3F–S3I). Activating CI neurons resulted in an immediate (≤1 s of stimulus) cessation of locomotion (Figure S3F; Movie S5) rather than CT (quantified as a change in body length) (Figure 3A). Optogenetic activation of CII neurons elicited CT, however activation of CIII produced a more robust and longer CT in more larvae (Figure 3B–3C; Figure S3G–S3H, S3J–S3K; Movie S5). Activation of CIV neurons elicited aversive rolling (Figure 3D; Figure S3I; Movie S5) as previously reported [17]. Optogenetic activation of md neurons did not increase HTR responses (Figure S3F–I), further validating our focus on CT. Together these data reinforce and extend our GCaMP observations, demonstrating that light-mediated activation of CIII, or CII, neurons is sufficient to generate CT responses.

Class III sensory neurons mediate cold-evoked CT behavior

We next examined whether CII, CIII, or other md neurons are required for cold-evoked CT. We electrically silenced md neurons via class-specific expression of tetanus toxin and examined their cold-evoked responses. In the cold plate assay, silencing CIII neurons significantly attenuated CT (Figure 4A). We also observed mild reductions in CT upon silencing CI neurons, however silencing CII or CIV neurons had no significant effect on cold-evoked CT (Figure S4A). In the cold probe assay, silencing CIII neurons also resulted in a significant reduction of CT (Figure 4B), while silencing CI, CII, or CIV resulted in no change in cold-evoked CT versus genetic controls (Figure S4B). Silencing CII and CIII neurons together (Figure S3E), resulted in mild to equivalent reductions in cold responses in the plate or probe assays respectively versus silencing CIII alone (Figure S4).

As an alternative approach we interfered with the *para* gene, which encodes a NaV type sodium channel, to block action potential propagation in CIII neurons [35, 36]. This blocked cold-induced CT in both assays (Figures 4C–4D). Together, these data support a prominent role for CIII neurons in mediating CT to noxious cold in *Drosophila* larvae. These results are consistent with the neuron-specific GCaMP responses (Figure 2) and optogenetic activation data (Figure 3) and support that cold-evoked CT is sensory neuron mediated.

The TRP channels Pkd2, Trpm, and NompC are expressed in class III md neurons

As TRP channels mediate diverse thermosensory responses in *Drosophila* and other animals [22], we hypothesized that cold-evoked CT might be mediated by one or more TRP channels expressed in CIII neurons. Whole genome microarray expression comparisons between isolated CIII neurons and whole larval extracts identified the TRP channels *nompC* and *Trpm* RF isoform as significantly enriched in CIII neurons (Figure 5A). Comparisons between CIII and CIV neurons revealed *Pkd2* and the *Trpm* RB isoform were specifically enriched in cold-responsive versus heat-responsive neurons (Figure 5A). Interestingly, while the *nompC* RD isoform was enriched in CIII neurons compared to whole larvae, isoform RA was enriched in both CIII and CIV compared to whole larvae (Figure 5A). Additionally, other TRP channel genes were found to be enriched in CIII vs CIV (Figure S5A).

Comparative qRT-PCR for *Pkd2*, *nompC*, and *Trpm* in isolated CIII or CIV neurons revealed significant enrichment of *nompC* and *Pkd2* in CIII neurons, however, *Trpm* expression showed only a mild increase which was not significant (Figure 5B). This latter case could be due to the amplicon used in the qRT-PCR analyses recognizing all *Trpm* isoforms, possibly masking class-specific enrichment (Figure 5B). A *nompC* promoter fragment driving Gal4 expression labels CIII neurons (Figure S3D) and NompC protein is expressed in CIII neuron filopodia [19, 20]. Collectively, these data suggest that *nompC, Trpm* and *Pkd2* are expressed in the proper cells to mediate cold-evoked behavior.

Pkd2, Trpm, and NompC function in class III neurons to respond to noxious cold

To test whether *nompC, Trpm* or *Pkd2* are required for noxious cold detection, we assayed mutants. Larvae bearing *Pkd2*, *Trpm* and *nompC* null alleles over relevant deficiencies had significantly reduced cold-evoked CT in both assays (Figure 5C–5D). Larvae expressing transheterozygous mutant alleles for these genes also showed CT defects (Figure S5B–S5C). Larvae expressing *UAS-RNAi* transgenes targeting *Pkd2*, *Trpm* or *nompC* in CIII neurons also showed significant decreases in CT (Figure 5C–5D). Targeted overexpression of either *nompC* or *Pkd2* in CIII neurons in a mutant background rescued these defects (Figures 5E–5F), with the exception of *nompC* in the cold plate assay. Importantly, disruption of *Pkd2, Trpm* or *nompC*, had no significant effect on CIII dendritic morphology (Figure S6). *nompC* has been implicated in both cold (here) and gentle touch [19, 20]. Thus we tested whether *Pkd2* and *Trpm* also affect gentle touch responsiveness. All three mutants had slight defects in gentle touch sensation (see Figure S7 and methods for assay details).

Roles of Pkd2, Trpm and NompC in sensing cold

Do the identified TRP channels function in general neuronal excitability or do they have a specific thermosensory function in detecting noxious cold? Upon CIII neuron optogenetic activation with TRP-specific RNAi expression, larvae still exhibited robust CT (Figure 6A). In contrast, when co-expressing RNAi targeting para, CT was blocked upon optogenetic activation (Figure 6A).

To determine if Pkd2, NompC or Trpm are required for the observed calcium increases in CIII neurons stimulated with cold, we measured CIII GCaMP responses in TRP channel mutants. In all three mutants, cold-induced calcium responses were altered (Figure 6B).

Cold-induced CIII calcium responses went up in Trpm mutants and down in Pkd2 mutants, while nompC mutants exhibited a slight, but non-significant, increase (Figures 6B–6C). These results suggest potentially complex roles for NompC and Trpm in regulating neuronal calcium homeostasis upon cold exposure and a more direct role for Pkd2 in cold sensing. Consistent with this, overexpressing Pkd2 in non-cold sensing CIV neurons resulted in a conferrence of GCaMP cold sensitivity (Figure 6D).

Class III-mediated multimodal behavior depends upon activation levels

Our results thus far implicate CIII neurons as cold sensors making them multimodal given their gentle touch function [19, 20]. One of the primary reactions to gentle touch is a head withdrawal (HW) [32, 33], which is like an asymmetric CT. To clarify how these cells might distinguish between cold and gentle touch we varied the dose of optogenetic light activating CIII neurons, to see if a particular activation level evoked either HW or CT (Figure 7A, Movie S6). Optogenetic activation of CIII neurons at the highest dose, resulted in CT almost exclusively (Figure 7A). The percentage of CT responders was reduced with decreasing light, however while HW responses increased (Figure 7A).

Our optogenetic dose-response suggests that cold may activate CIII neurons more strongly than light touch or activate more CIII neurons. To investigate this, we utilized the genetic tool CaMPARI, which upon exposure to photoconverting violet light shifts fluorescence from green to red as a function of intracellular calcium levels evoked by a specific stimulus [37] (Figures 7B–7D). CIII neurons expressing CaMPARI exhibited a significant increase in photoconversion in response to cold versus gentle touch (Figures 7B–7D). While a similar number of activated CIII neurons were observed between cold and gentle touch stimulated larvae, cold evoked significantly larger CaMPARI responses in multiple larval segments (Figures 7B–7D). These data suggest that noxious cold more strongly activates CIII neurons compared to gentle touch.

Coactivation of thermosensory nociceptors results in predominantly cold-evoked responses

CIII and CIV dendritic arbors extensively tile the epidermis and their axonal projections terminate near each other in the anterior ventral nerve cord [16, 38]. To understand how cold and hot stimuli are sensed, we asked what behavioral output would be observed upon directly stimulating CIII (CT) and CIV (BR) neurons simultaneously. Optogentic coactivation of CIII and CIV neurons in live larvae produced exclusively CT (Figure 7E; Movie S7).

Additionally, we tried an alternative approach to address possible thermosensory competition between neuron types. TrpA1 expression has been used to thermogenetically activate non-thermosensory neurons [39]. Therefore, applying a heat probe to larvae over-expressing the warm-activated TRPA1 channel in CIII neurons should activate these neurons and endogenous CIV heat-sensitive channels. Similar to above, simultaneous CIII and CIV activation in this manner resulted in predominantly CT, correlated with a dramatic reduction in the typical level of heat-evoked BR responses (Figure 7F). These results suggest that

noxious cold signals and subsequent CT overrides signals from noxious heat and BR responses when CIII and CIV neurons are simultaneously activated.

DISCUSSION

We developed assays to identify the cells and channels required to respond to noxious cold. The primary cold-evoked behavior, CT, is unlike larval responses to other types of nociceptive [11, 13, 17, 18, 24] and innocuous stimuli [19, 20, 32, 33]. Several lines of evidence indicate that CIII neurons are cold nociceptors. First, CIII neurons are directly and specifically activated by cold temperatures. Second, CIII neurons directly reproduce a robust CT in larvae upon strong optogenetic activation. Lastly, these neurons are required to produce a robust cold-evoked CT response, rather than the highly multimodal CIV neurons that mediate responses to heat [17, 24], harsh touch [13, 18], and UV light [40].

Multiple lines of evidence suggest how CIII neurons may be activated by both noxious cold (this study) and gentle touch [19, 20]. First, when CIII neurons are optogenetically stimulated with low doses of light larvae exhibit a gentle touch behavior (HW), while stronger doses of light resulted in CT. Second, CaMPARI analysis indicates a significant difference between the magnitude of CIII activation when larvae are stimulated with noxious cold versus gentle touch. These data suggest that CIII neurons may have different activation thresholds that ultimately determine the correct behavioral output to different stimuli. This is an important finding since until now it has remained an open question how multimodal neurons detect different types of stimuli to induce varying behavioral responses. For example, it is unknown how CIV neurons mediate behavioral responses to high temperature/harsh touch (BR) versus proprioceptive feedback (normal locomotion) [41, 42]. The optogenetic dose-response strategy used here could be useful for any case where a single neuron gives two distinguishable behavioral outputs.

At the molecular level, *Pkd2*, *nompC*, and *Trpm*, are enriched and appear to function in CIII neurons to mediate cold-evoked CT. This indicates that these channels are multimodal given their other known sensory functions; such as *nompC* in gentle touch [19, 20], and *Pkd2* in taste [43, 44] and mechanosensation in the primary cilia of the vertebrate kidney epithelium [45]. This latter function may be related to the role of *Pkd2* in autosomal dominant polycystic kidney disease [46]. Currently, it is unclear if patients suffering from this disease, or mice lacking the gene [47], have cold nociception defects. Lastly, although TRPM8 acts as a cold sensor in vertebrates [8, 48], it maintains zinc and magnesium homeostasis [49, 50] in *Drosophila*, and ours is the first evidence that a *Trpm* family member acts in cold nociception in *Drosophila.*

While multimodality is common among TRPs and other channels (see painless [12, 24, 51]; dTRPA1 [12, 40, 52–54]; Pickpocket1 [41, 42, 51] and Pickpocket 26 [42, 55]), it begs the question: how do these channels distinguish between innocuous and harsh stimuli? For *painless* and *dTRPA1,* splice variants may function differently [56]. For *nompC*, ankyrin repeats are important for its mechanosensory function [57, 58] and it will be interesting to determine whether this is also true for cold sensation. Other studies suggest TRP channels may collaborate with different sets of partially overlapping channels for different functions.

For gentle touch, this appears to include NompC, Ripped Pocket, Nmdar1 and Nmdar2 [19, 20]. For noxious cold, vertebrate studies revealed interactions between TRPM8 and potassium channels (Task-3, Kv1 and Kv7) (see review [59]). Such potential interactions may help explain how increased GCaMP responses to cold in *Trpm* mutants could lead to inhibition of cold-evoked behavior. Altered cold-evoked GCaMP responses could suggest that these channels work in tandem with other channels, such as calcium-activated potassium channels, to regulate cellular and behavioral cold responses. Excess calcium in *Trpm* mutants could lead to activation of calcium-activated potassium channels and thereby promote hyperpolarization, which would contribute to inhibition of CT behavior. In fact, when microarray expression profiles of CIII versus CIV neurons were examined, two particular calcium-activated potassium channels were found to be enriched in CIII neurons (SK, 2.1 average fold change and slowpoke, 10.4 average fold change; see GEO accessions GSE69353 and GSE46154). Altered calcium responses in *Trpm* and *Pkd2* mutants may also indicate that cold-evoked behavior is sensitive to optimal calcium levels, such that above or below these levels, the behavior is inhibited. Other models are also conceivable. Of the TRP channels identified here, Pkd2 seems the most likely to act as a direct cold sensor as calcium levels are decreased upon cold exposure in *Pkd2* mutants and misexpression of Pkd2 confers cold-responsiveness to other sensory neurons.

In adults and larvae, *Drosophila* avoid temperatures outside their comfortable range by utilizing a distinct set of thermosensitive antennal or dorsal organ neurons in the head [31, 60]. Interestingly, the cold sensitive neurons are inhibited by heat and vice versa; ultimately, these thermosensory circuits determine motor output to help the animal navigate along a temperature gradient [31, 60]. Similar circuits have begun to be characterized for noxious stimuli [61, 62]. Here, coactivation of hot (CIV) and cold (CIII) neurons provokes a dominant CT that is unlikely to arise solely from faster neuronal conduction since both neurons terminate at similar locations in the anterior ventral nerve cord [38]. It is not known whether CIII neurons, like CIV, converge onto basin interneurons [61], but unraveling the architecture of this circuit will be an interesting avenue for future work. We suspect that optogenetic coactivation and CaMPARI techniques, as used here, will be valuable tools in this endeavor.

Taken together, our results identify the peripheral sensory neurons responsible for noxious cold detection in *Drosophila* larvae and conserved molecular players required for this process. The cold assays we have developed offer powerful models for the genetic dissection of cold nociception. Further exploitation of these models should yield exciting insight into cold nociceptive circuitry.

EXPERIMENTAL PROCEDURES

For detailed methods, see Supplemental Experimental Procedures.

Behavioral Assays

In all behavioral assays, freely moving mid 3rd instar larvae were used, age-matched and selected based on size. In the cold probe assay, larvae were placed under a brightfield stereomicroscope (Zeiss Stemi 2000). The tip of the custom-built probe (ProDev

Engineering, Figure 1C) was gently placed on the dorsal midline (segment A4) and held for either 10 s or until the first behavioral response. Larvae that did not respond within 10 s were recorded as non-responders. In the cold plate assay, larvae were placed ventral side down on a 25 °C thin metal plate (2 mm) coated with a fine mist of water. The metal plate was transferred to a Peltier-controlled plate preset to between 4–16 °C (Figure 1A) as verified with a Fluke 62 mini infrared thermometer and responses were recorded (See supplemental Experimental Procedures). For both assays cold-evoked behaviors precluded normal locomotion and each larva was only stimulated once (except Figure S1E). In all *GAL4/UAS* experiments, transgenes were heterozygous and no balancers or markers were present in the larvae tested. Unless otherwise stated, statistical analysis of behavior consisted of *two-tailed Fisher's Exact test with Bonferonni corrections.*

Supplementary Material

Refer to Web version on PubMed Central for supplementary material.

Acknowledgments

This research was supported by NIH National Institute of Child Health and Human Development Training Grant (NIH T32-HD07325), NIH Predoctoral Kirschstein NRSA Fellowship (NINDS F31 NS083306) and the Marilyn and Frederick R. Lummis, Jr. MD Fellowship (HNT), as well as a 2CI Neurogenomics Fellowship (AAP). The Galko laboratory is supported by NINDS R01 NS069828 and NINDS R21 NS087360. The Cox laboratory is supported by NINDS R01 NS086082, NIMH R15 MH086928, GSU Brains & Behavior Seed Grant, and a 4-VA Innovation Award. We acknowledge Bloomington *Drosophila* (NIH P40ODO18537), NIG-Fly Japan, and VDRC stock centers for fly stocks as well as Kartik Venkatachalam, Dan Tracey, Paul Garrity, Hugo Bellen, Michael Welsh, Michael Stern, Steve Stowers, Xiangyi Lu, and Yuh-Nung Jan. We thank Cox lab member Ravi Das for technical assistance with whole mount confocal imaging, former Galko lab member Sarah Wu for initial cold probe assay development, and members of the Galko and Cox labs for critical evaluation of the manuscript.

References

1. Hayward JS, Eckerson JD, Collis ML. Effect of behavioral variables on cooling rate of man in cold water. J Appl Physiol. 1975; 38:1073–1077. [PubMed: 1141120]
2. Pinshow B, Fedak MA, Battles DR, Schmidt-Nielsen K. Energy expenditure for thermoregulation and locomotion in emperor penguins. Am J Physiol. 1976; 231:903–912. [PubMed: 970474]
3. Bonoan RE, Goldman RR, Wong PY, Starks PT. Vasculature of the hive: heat dissipation in the honey bee (Apis mellifera) hive. Naturwissenschaften. 2014; 101:459–465. [PubMed: 24760416]
4. Jasmin L, Kohan L, Franssen M, Janni G, Goff JR. The cold plate as a test of nociceptive behaviors: description and application to the study of chronic neuropathic and inflammatory pain models. Pain. 1998; 75:367–382. [PubMed: 9583773]
5. Pizziketti RJ, Pressman NS, Geller EB, Cowan A, Adler MW. Rat cold water tail-flick: a novel analgesic test that distinguishes opioid agonists from mixed agonist-antagonists. Eur J Pharmacol. 1985; 119:23–29. [PubMed: 2867920]
6. Choi Y, Yoon YW, Na HS, Kim SH, Chung JM. Behavioral signs of ongoing pain and cold allodynia in a rat model of neuropathic pain. Pain. 1994; 59:369–376. [PubMed: 7708411]
7. Brenner DS, Golden JP, Gereau RWt. A novel behavioral assay for measuring cold sensation in mice. PLoS One. 2012; 7:e39765. [PubMed: 22745825]
8. Dhaka A, Murray AN, Mathur J, Earley TJ, Petrus MJ, Patapoutian A. TRPM8 is required for cold sensation in mice. Neuron. 2007; 54:371–378. [PubMed: 17481391]
9. Kwan KY, Allchorne AJ, Vollrath MA, Christensen AP, Zhang DS, Woolf CJ, Corey DP. TRPA1 contributes to cold, mechanical, and chemical nociception but is not essential for hair-cell transduction. Neuron. 2006; 50:277–289. [PubMed: 16630838]

10. Bellen HJ, Tong C, Tsuda H. 100 years of Drosophila research and its impact on vertebrate neuroscience: a history lesson for the future. Nat Rev Neurosci. 2010; 11:514–522. [PubMed: 20383202]
11. Babcock DT, Landry C, Galko MJ. Cytokine signaling mediates UV-induced nociceptive sensitization in Drosophila larvae. Curr Biol. 2009; 19:799–806. [PubMed: 19375319]
12. Babcock DT, Shi S, Jo J, Shaw M, Gutstein HB, Galko MJ. Hedgehog signaling regulates nociceptive sensitization. Curr Biol. 2011; 21:1525–1533. [PubMed: 21906949]
13. Kim SE, Coste B, Chadha A, Cook B, Patapoutian A. The role of Drosophila Piezo in mechanical nociception. Nature. 2012; 483:209–212. [PubMed: 22343891]
14. Neely GG, Rao S, Costigan M, Mair N, Racz I, Milinkeviciute G, Meixner A, Nayanala S, Griffin RS, Belfer I, et al. Construction of a global pain systems network highlights phospholipid signaling as a regulator of heat nociception. PLoS Genet. 2012; 8:e1003071. [PubMed: 23236288]
15. Takeuchi K, Nakano Y, Kato U, Kaneda M, Aizu M, Awano W, Yonemura S, Kiyonaka S, Mori Y, Yamamoto D, et al. Changes in temperature preferences and energy homeostasis in dystroglycan mutants. Science. 2009; 323:1740–1743. [PubMed: 19325118]
16. Grueber WB, Jan LY, Jan YN. Tiling of the Drosophila epidermis by multidendritic sensory neurons. Development. 2002; 129:2867–2878. [PubMed: 12050135]
17. Hwang RY, Zhong L, Xu Y, Johnson T, Zhang F, Deisseroth K, Tracey WD. Nociceptive neurons protect Drosophila larvae from parasitoid wasps. Curr Biol. 2007; 17:2105–2116. [PubMed: 18060782]
18. Zhong L, Hwang RY, Tracey WD. Pickpocket is a DEG/ENaC protein required for mechanical nociception in Drosophila larvae. Curr Biol. 2010; 20:429–434. [PubMed: 20171104]
19. Tsubouchi A, Caldwell JC, Tracey WD. Dendritic filopodia, Ripped Pocket, NOMPC, and NMDARs contribute to the sense of touch in Drosophila larvae. Curr Biol. 2012; 22:2124–2134. [PubMed: 23103192]
20. Yan Z, Zhang W, He Y, Gorczyca D, Xiang Y, Cheng LE, Meltzer S, Jan LY, Jan YN. Drosophila NOMPC is a mechanotransduction channel subunit for gentle-touch sensation. Nature. 2013; 493:221–225. [PubMed: 23222543]
21. Simone DA, Kajander KC. Excitation of rat cutaneous nociceptors by noxious cold. Neurosci Lett. 1996; 213:53–56. [PubMed: 8844711]
22. Venkatachalam K, Montell C. TRP channels. Annu Rev Biochem. 2007; 76:387–417. [PubMed: 17579562]
23. Caterina MJ, Schumacher MA, Tominaga M, Rosen TA, Levine JD, Julius D. The capsaicin receptor: a heat-activated ion channel in the pain pathway. Nature. 1997; 389:816–824. [PubMed: 9349813]
24. Tracey WD Jr, Wilson RI, Laurent G, Benzer S. painless, a Drosophila gene essential for nociception. Cell. 2003; 113:261–273. [PubMed: 12705873]
25. Sarria I, Ling J, Xu GY, Gu JG. Sensory discrimination between innocuous and noxious cold by TRPM8-expressing DRG neurons of rats. Mol Pain. 2012; 8:79. [PubMed: 23092296]
26. Story GM, Peier AM, Reeve AJ, Eid SR, Mosbacher J, Hricik TR, Earley TJ, Hergarden AC, Andersson DA, Hwang SW, et al. ANKTM1, a TRP-like channel expressed in nociceptive neurons, is activated by cold temperatures. Cell. 2003; 112:819–829. [PubMed: 12654248]
27. Munns C, AlQatari M, Koltzenburg M. Many cold sensitive peripheral neurons of the mouse do not express TRPM8 or TRPA1. Cell Calcium. 2007; 41:331–342. [PubMed: 16949152]
28. Garrity PA, Goodman MB, Samuel AD, Sengupta P. Running hot and cold: behavioral strategies, neural circuits, and the molecular machinery for thermotaxis in C. elegans and Drosophila. Genes Dev. 2010; 24:2365–2382. [PubMed: 21041406]
29. Rosenzweig M, Kang K, Garrity PA. Distinct TRP channels are required for warm and cool avoidance in Drosophila melanogaster. Proc Natl Acad Sci U S A. 2008; 105:14668–14673. [PubMed: 18787131]
30. Kwon Y, Shen WL, Shim HS, Montell C. Fine thermotactic discrimination between the optimal and slightly cooler temperatures via a TRPV channel in chordotonal neurons. J Neurosci. 2010; 30:10465–10471. [PubMed: 20685989]

31. Gallio M, Ofstad TA, Macpherson LJ, Wang JW, Zuker CS. The coding of temperature in the Drosophila brain. Cell. 2011; 144:614–624. [PubMed: 21335241]
32. Kernan M, Cowan D, Zuker C. Genetic dissection of mechanosensory transduction: mechanoreception-defective mutations of Drosophila. Neuron. 1994; 12:1195–1206. [PubMed: 8011334]
33. Zhou Y, Cameron S, Chang WT, Rao Y. Control of directional change after mechanical stimulation in Drosophila. Mol Brain. 2012; 5:39. [PubMed: 23107101]
34. Jeacocke RE. Calcium efflux during the cold-induced contraction of mammalian striated muscle fibres. Biochim Biophys Acta. 1982; 682:238–244. [PubMed: 7171581]
35. Loughney K, Kreber R, Ganetzky B. Molecular analysis of the para locus, a sodium channel gene in Drosophila. Cell. 1989; 58:1143–1154. [PubMed: 2550145]
36. O'Dowd DK, Germeraad SE, Aldrich RW. Alterations in the expression and gating of Drosophila sodium channels by mutations in the para gene. Neuron. 1989; 2:1301–1311. [PubMed: 2560637]
37. Fosque BF, Sun Y, Dana H, Yang CT, Ohyama T, Tadross MR, Patel R, Zlatic M, Kim DS, Ahrens MB, et al. Neural circuits. Labeling of active neural circuits in vivo with designed calcium integrators. Science. 2015; 347:755–760. [PubMed: 25678659]
38. Grueber WB, Ye B, Yang CH, Younger S, Borden K, Jan LY, Jan YN. Projections of Drosophila multidendritic neurons in the central nervous system: links with peripheral dendrite morphology. Development. 2007; 134:55–64. [PubMed: 17164414]
39. Hamada FN, Rosenzweig M, Kang K, Pulver SR, Ghezzi A, Jegla TJ, Garrity PA. An internal thermal sensor controlling temperature preference in Drosophila. Nature. 2008; 454:217–220. [PubMed: 18548007]
40. Xiang Y, Yuan Q, Vogt N, Looger LL, Jan LY, Jan YN. Light-avoidance-mediating photoreceptors tile the Drosophila larval body wall. Nature. 2010; 468:921–926. [PubMed: 21068723]
41. Ainsley JA, Pettus JM, Bosenko D, Gerstein CE, Zinkevich N, Anderson MG, Adams CM, Welsh MJ, Johnson WA. Enhanced locomotion caused by loss of the Drosophila DEG/ENaC protein Pickpocket1. Curr Biol. 2003; 13:1557–1563. [PubMed: 12956960]
42. Gorczyca DA, Younger S, Meltzer S, Kim SE, Cheng L, Song W, Lee HY, Jan LY, Jan YN. Identification of Ppk26, a DEG/ENaC Channel Functioning with Ppk1 in a Mutually Dependent Manner to Guide Locomotion Behavior in Drosophila. Cell Rep. 2014; 9:1446–1458. [PubMed: 25456135]
43. Ishimaru Y, Inada H, Kubota M, Zhuang H, Tominaga M, Matsunami H. Transient receptor potential family members PKD1L3 and PKD2L1 form a candidate sour taste receptor. Proc Natl Acad Sci U S A. 2006; 103:12569–12574. [PubMed: 16891422]
44. Huang AL, Chen X, Hoon MA, Chandrashekar J, Guo W, Trankner D, Ryba NJ, Zuker CS. The cells and logic for mammalian sour taste detection. Nature. 2006; 442:934–938. [PubMed: 16929298]
45. Nauli SM, Alenghat FJ, Luo Y, Williams E, Vassilev P, Li X, Elia AE, Lu W, Brown EM, Quinn SJ, et al. Polycystins 1 and 2 mediate mechanosensation in the primary cilium of kidney cells. Nat Genet. 2003; 33:129–137. [PubMed: 12514735]
46. Mochizuki T, Wu G, Hayashi T, Xenophontos SL, Veldhuisen B, Saris JJ, Reynolds DM, Cai Y, Gabow PA, Pierides A, et al. PKD2, a gene for polycystic kidney disease that encodes an integral membrane protein. Science. 1996; 272:1339–1342. [PubMed: 8650545]
47. Wu G, D'Agati V, Cai Y, Markowitz G, Park JH, Reynolds DM, Maeda Y, Le TC, Hou H Jr, Kucherlapati R, et al. Somatic inactivation of Pkd2 results in polycystic kidney disease. Cell. 1998; 93:177–188. [PubMed: 9568711]
48. Peier AM, Moqrich A, Hergarden AC, Reeve AJ, Andersson DA, Story GM, Earley TJ, Dragoni I, McIntyre P, Bevan S, et al. A TRP channel that senses cold stimuli and menthol. Cell. 2002; 108:705–715. [PubMed: 11893340]
49. Hofmann T, Chubanov V, Chen X, Dietz AS, Gudermann T, Montell C. Drosophila TRPM channel is essential for the control of extracellular magnesium levels. PLoS One. 2010; 5:e10519. [PubMed: 20463899]

50. Georgiev P, Okkenhaug H, Drews A, Wright D, Lambert S, Flick M, Carta V, Martel C, Oberwinkler J, Raghu P. TRPM channels mediate zinc homeostasis and cellular growth during Drosophila larval development. Cell Metab. 2010; 12:386–397. [PubMed: 20889130]
51. Johnson WA, Carder JW. Drosophila nociceptors mediate larval aversion to dry surface environments utilizing both the painless TRP channel and the DEG/ENaC subunit, PPK1. PLoS One. 2012; 7:e32878. [PubMed: 22403719]
52. Neely GG, Keene AC, Duchek P, Chang EC, Wang QP, Aksoy YA, Rosenzweig M, Costigan M, Woolf CJ, Garrity PA, et al. TrpA1 regulates thermal nociception in Drosophila. PLoS One. 2011; 6:e24343. [PubMed: 21909389]
53. Kang K, Pulver SR, Panzano VC, Chang EC, Griffith LC, Theobald DL, Garrity PA. Analysis of Drosophila TRPA1 reveals an ancient origin for human chemical nociception. Nature. 2010; 464:597–600. [PubMed: 20237474]
54. Kim SH, Lee Y, Akitake B, Woodward OM, Guggino WB, Montell C. Drosophila TRPA1 channel mediates chemical avoidance in gustatory receptor neurons. Proc Natl Acad Sci U S A. 2010; 107:8440–8445. [PubMed: 20404155]
55. Guo Y, Wang Y, Wang Q, Wang Z. The role of PPK26 in Drosophila larval mechanical nociception. Cell Rep. 2014; 9:1183–1190. [PubMed: 25457610]
56. Zhong L, Bellemer A, Yan H, Ken H, Jessica R, Hwang RY, Pitt GS, Tracey WD. Thermosensory and nonthermosensory isoforms of Drosophila melanogaster TRPA1 reveal heat-sensor domains of a thermoTRP Channel. Cell Rep. 2012; 1:43–55. [PubMed: 22347718]
57. Hwang RY, Stearns NA, Tracey WD. The ankyrin repeat domain of the TRPA protein painless is important for thermal nociception but not mechanical nociception. PLoS One. 2012; 7:e30090. [PubMed: 22295071]
58. Zhang W, Cheng LE, Kittelmann M, Li J, Petkovic M, Cheng T, Jin P, Guo Z, Gopfert MC, Jan LY, et al. Ankyrin Repeats Convey Force to Gate the NOMPC Mechanotransduction Channel. Cell. 2015; 162:1391–1403. [PubMed: 26359990]
59. Wang H, Siemens J. TRP ion channels in thermosensation, thermoregulation and metabolism. Temperature (Austin). 2015; 2:178–187. [PubMed: 27227022]
60. Klein M, Afonso B, Vonner AJ, Hernandez-Nunez L, Berck M, Tabone CJ, Kane EA, Pieribone VA, Nitabach MN, Cardona A, et al. Sensory determinants of behavioral dynamics in Drosophila thermotaxis. Proc Natl Acad Sci U S A. 2015; 112:E220–229. [PubMed: 25550513]
61. Ohyama T, Schneider-Mizell CM, Fetter RD, Aleman JV, Franconville R, Rivera-Alba M, Mensh BD, Branson KM, Simpson JH, Truman JW, et al. A multilevel multimodal circuit enhances action selection in Drosophila. Nature. 2015; 520:633–639. [PubMed: 25896325]
62. Frank DD, Jouandet GC, Kearney PJ, Macpherson LJ, Gallio M. Temperature representation in the Drosophila brain. Nature. 2015; 519:358–361. [PubMed: 25739506]

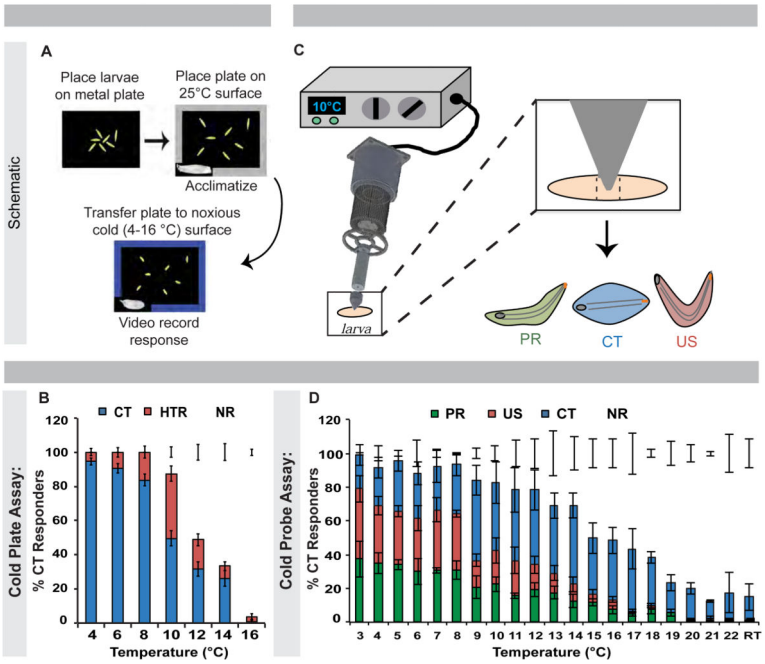

Figure 1. *Drosophila* larvae have unique behavioral responses to noxious cold stimuli

(A) Diagram of and (B) averaged responses versus temperature in cold plate assay. Error bars: ± s.e.p., n = 96–119. (C) Diagram of cold probe assay. (D) Larval response versus temperature in cold probe assay averaged ± s.e.m., n = 120. (B-D) HTR = head and/or tail raise, US = U-Shape; CT = Contraction; PR = Posterior raise; NR = No response; RT = room temperature. See also Figure S1 and Movies S1–S3.

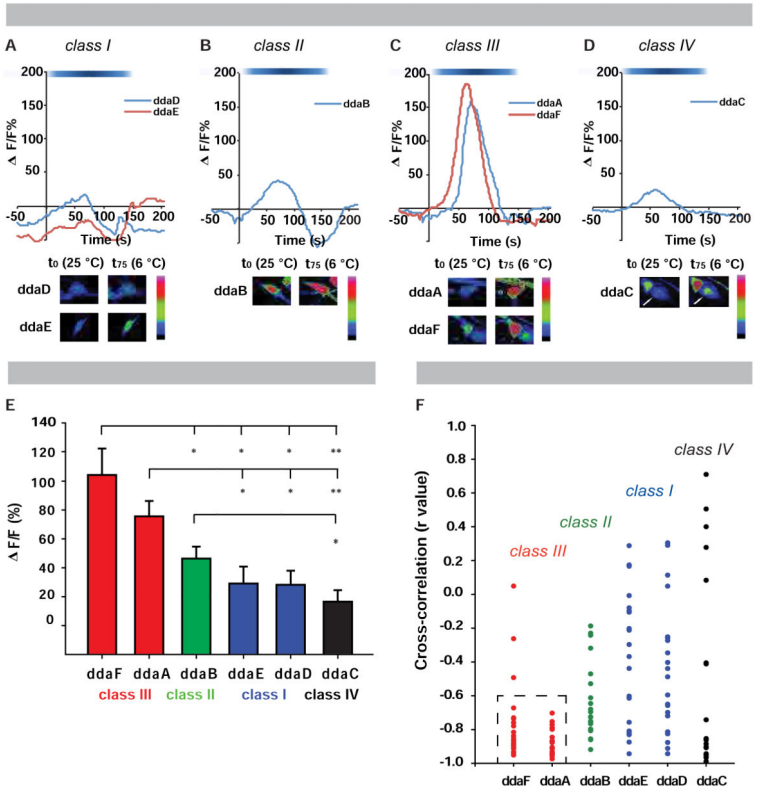

Figure 2. Class II and III sensory neurons are activated by cold

((A–D) Representative tracings of class-specific GCaMP6 responses (ΔF/F) with cold stimulation (6 °C) in (A) CI (ddaD, ddaE), (B) CII (ddaB), (C) CIII (ddaA, ddaF), and (D) CIV neurons (ddaC, marked by white arrow). (A–D) White-blue spectrum bar signifies temperature range (25–6 °C). Bottom inserts: neuronal activation at a cold temperature (6 °C) and baseline temperature (25 °C). (E) Average peak change in fluorescence (ΔF/F) ± s.e.m., * = $p < 0.01$, ** = $p < 0.001$. (F) Cross-correlation analysis of neuronal activation with respect to temperature. Dashed box: clustered negative cross-correlation values for CIII neurons. (E–F) n = 20 per neuron. See also Figure S2 and Movie S4.

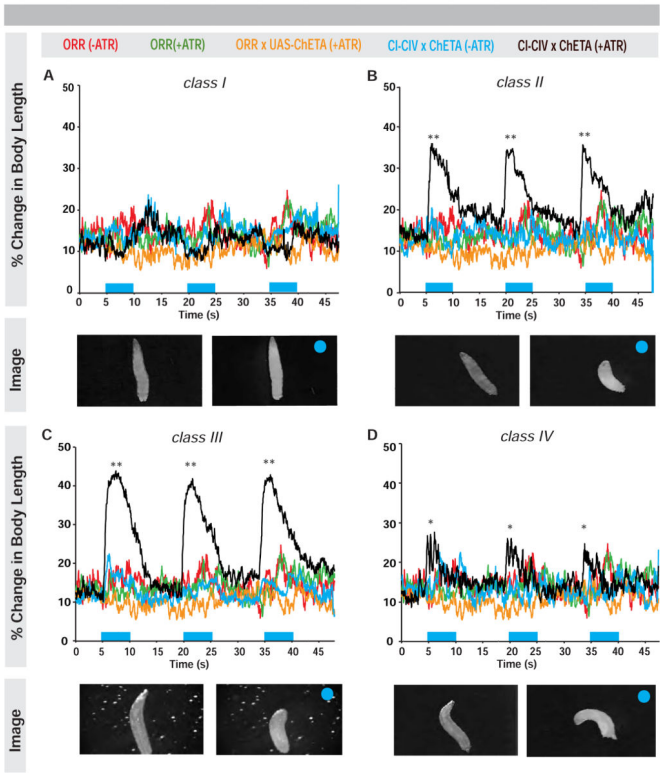

Figure 3. Optogenetic activation of class II and III neurons results in contract response

(Average percent change in body length over time upon light exposure (blue bars) and optogenetic activation (black) of (A) CI (B) CII (C) CIII or (D) CIV neurons. Larvae not fed (red) or fed (green) ATR, larvae bearing the UAS-channelrhodopsin transgene (ChETA) alone (orange), or larvae expressing ChETA but not fed ATR (blue) acted as negative controls. Bottom inserts: larval images of optogenetic activation for each class pre- and post-light (blue circle) exposure. * = $p < 0.05$, ** = $p < 0.01$, n = 15–20. See also Figure S3 and Movie S5.

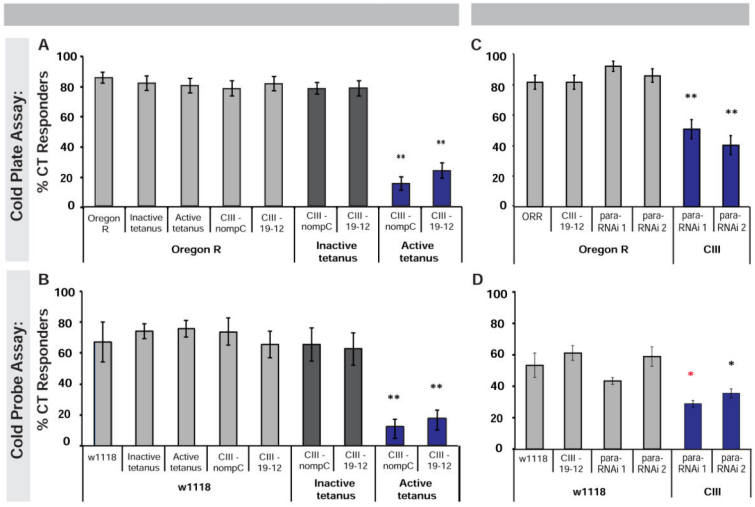

Figure 4. Class III sensory neurons mediate cold-evoked CT behavior

(Larvae with CIII neurons silenced via two independent drivers (nompC-GAL4 or 19–12-GAL4) were tested in the (A) cold plate (6 °C, n = 60–100 averaged ± s.e.p.) and (B) cold probe assay (11 °C, n = 180 averaged ± s.e.m.). (C–D) Larvae with CIII neurons expressing para-RNAi transgenes in (C) cold plate (6 °C, n = 62–71 averaged ± s.e.p.), and (D) cold probe assay (10 °C, n = 90 averaged ± s.e.m.). (A–D) white and grey bars indicate controls, blue bars indicate experimental results. * = $p < 0.05$, ** = $p < 0.0125$, * $p < 0.05$ compared to w1118 and CIII Gal4 control. See also Figure S4.

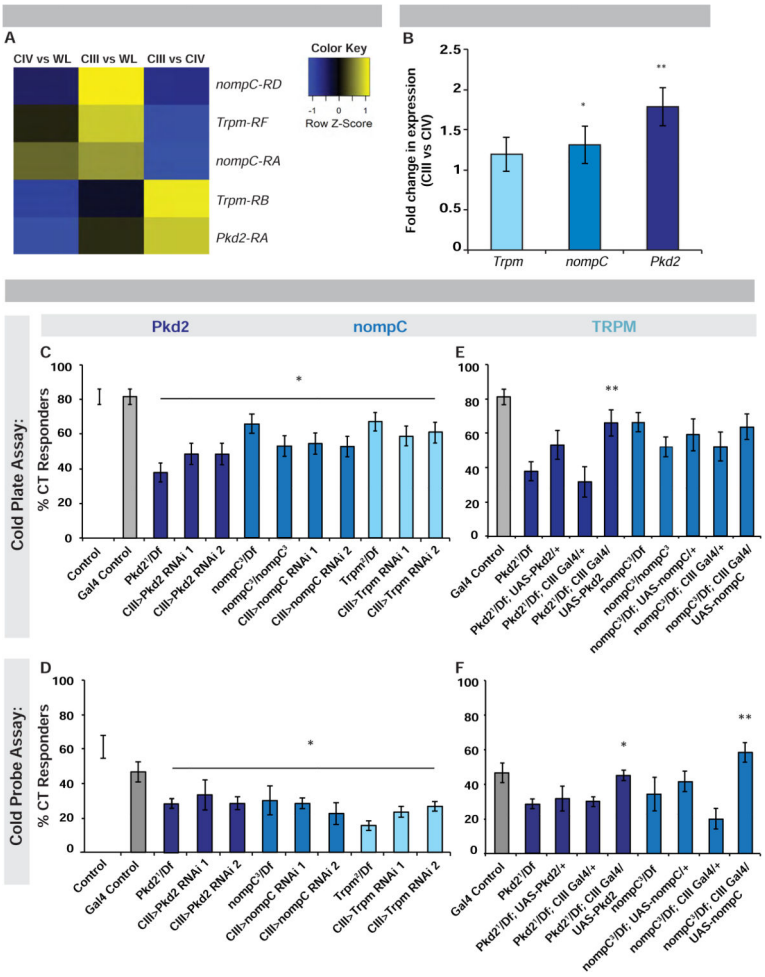

Figure 5. Expression and Function of TRP channels *Pkd2*, *Trpm* and *nompC* in class III sensory neurons

(A) Microarray comparing Pkd2, Trpm, and nompC isoforms in CIII vs. CIV neurons, CIII vs. whole larva (WL) or CIV vs. WL. Color key: degree of enrichment, yellow being more enriched and blue not enriched by comparison. n = 3. (B) qRT-PCR analysis of Pkd2, Trpm and nompC expression in CIII neurons vs. CIV. n = 4, values averaged ± s.e.p.. (C) Pkd2, nompC and Trpm mutant and targeted expression of RNAi transgenes in CIII in the cold plate (6 °C) and (D) cold probe (10 °C) assay. (E) Rescue of Pkd2 or nompC in CIII neurons via TRP overexpression in mutant over deficiency background in cold plate and (F) cold probe assay. (C) n = 60–81, responders averaged ± s.e.p.. (D) n = 90–120, responders averaged ± s.e.m.. (E) n = 22–74, responders averaged ± s.e.p.. (F) n = 3 sets of n = 20 averaged ± s.e.m.. (B–F) White and grey bars: controls; colored bars: different genes targeted. * = $p < 0.05$, ** = $p < 0.01$ (E, F) indicating significant compared to relevant mutant over deficiency control. See also Figure S5 and Figure S6.

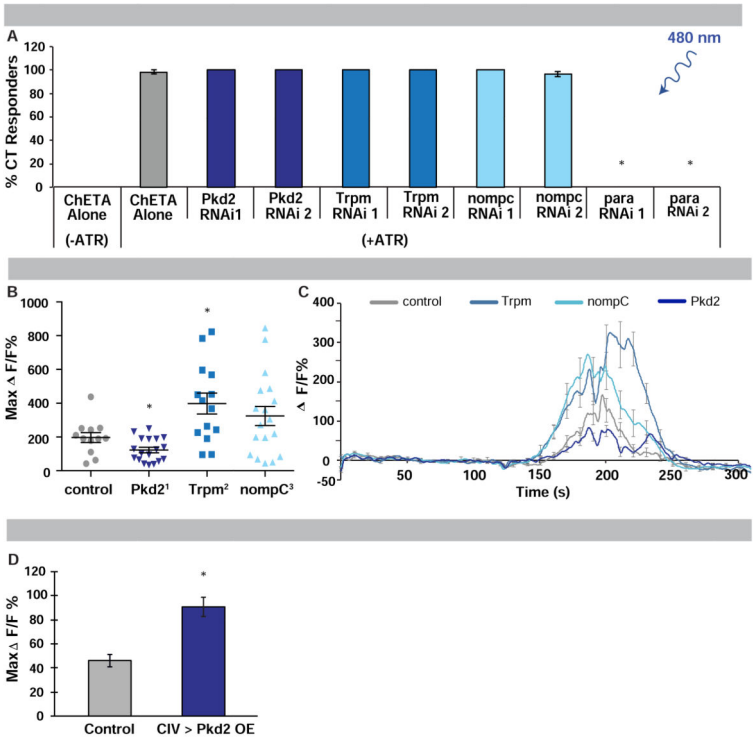

Figure 6. Role of Pkd2, Trpm and NompC in cold detection

(A) Responses to optogenetic activation of CIII expressing ChETA and RNAi transgenes with (+) or without (−) ATR. n = 60 averaged ± s.e.p.. * = $p < 0.0001$. (B) Maximum cold-induced change in GCaMP fluorescence in CIII neurons of TRP mutants, n = 12–18, error bars indicate s.e.m.. * = $p < 0.05$. (C) Averaged cold-induced change in GCaMP fluorescence in CIII neurons of TRP mutants over time, n = 12–14, error bars indicate s.e.m.. (D) Cold-evoked (6 °C) GCaMP response in CIV sensory neurons with targeted expression of Pkd2, n = 18 averaged ± s.e.m.. * = $p < 0.0001$. (A–D) Controls labeled in grey; specific genes targeted labeled in blues.

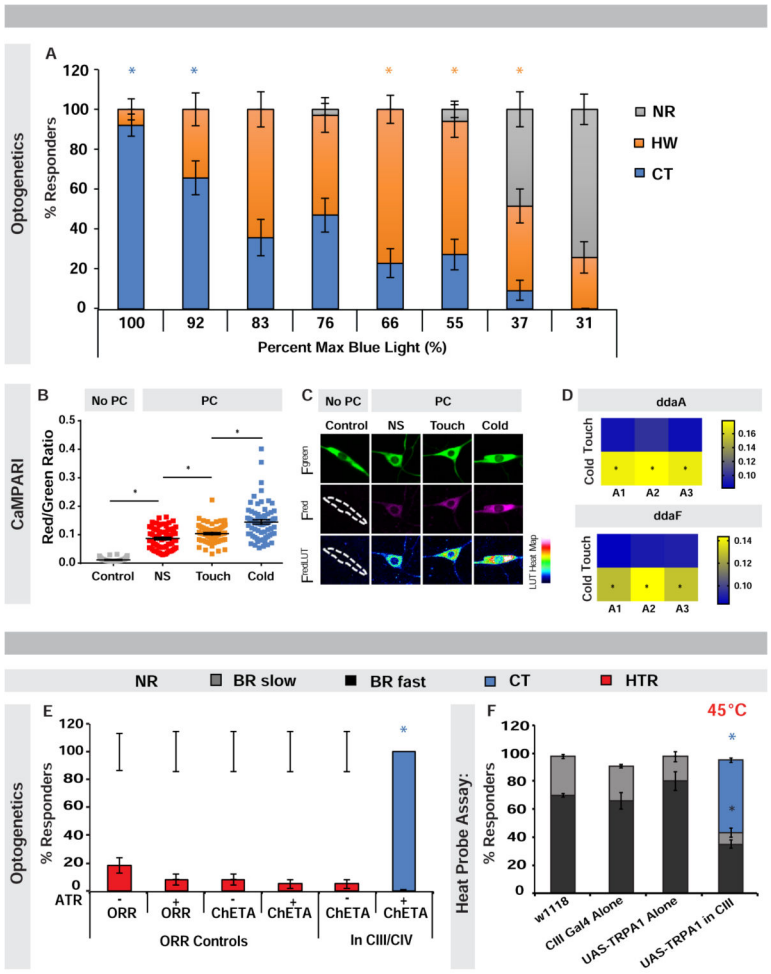

Figure 7. Optogenetic dose-response and coactivation experiments reveal how different output behaviors are determined

(A) Percent responders with varying light dose in larvae with CIII ChETA expression. n = 25–35 averaged ± s.e.p.. Colored *: significance of indicated behavior compared to other behaviors at given light dose. Blue * p = ≤ 0.02; orange * p = ≤ 0.004. (B) Ratio of CIII green to red photoconversion (PC) in non-PC (grey) and PC non-stimulated (NS) (red) controls vs. PC touch-stimulated (orange) and cold-stimulated (blue) larvae bearing CaMPARI transgenes, n = 70–72 averaged ± s.e.m.. * = $p < 0.01$. (C) Representative images of CIII neuron PC. (D) PC ratio heat map analysis (n = 9–12 animals), yellow indicating stronger PC in abdominal segments A1–A3. * = $p < 0.05$. (E) Percent responders upon CIII and CIV optogenetic coactivation. n = 45–60 averaged ± s.e.p.. * = $p < 0.001$. (F) Percent responders with CIII and CIV coactivation via CIII TRPA1 expression and heat probe stimulation (45 °C). n = 120 averaged ± s.e.m.. * p = < 0.001, colored * indicate significance between bars of same color. (A, E–F) CT = contraction; HW = head withdrawal; HTR = head and/or tail raise; BR fast = body roll within 5 s; BR slow = body roll with 6–20 s; NR = non-responder. See also Figure S7, and Movies S6 and S7.